6-2012

Secondary Droplet Breakup in Periodic Aerodynamic Flows using Computational Fluid Dynamics

Krystle Gallo
Union College - Schenectady, NY

Secondary Droplet Breakup in Periodic Aerodynamic Flows using Computational Fluid Dynamics

Krystle Gallo
Mechanical Engineering
Union College
Eight-Hundred Seven Union St
Schenectady, New York 12308 USA

Faculty Advisor: Bradford Bruno, Ph.D.

Abstract

Combustion instability is characterized by periodic fluctuations during the combustion process. Such instabilities can cause a reduction in engine performance and damage to engine components. In liquid fueled combustion, some types of combustion instability may be driven by changes in fuel droplet size distribution. The fuel droplet size distribution can be changed if the original or "primary" fuel droplets are broken apart by the flow. This is called secondary droplet breakup. The smaller drops that are created during breakup are consumed more rapidly and increase the energy release rate, which may act as a sustaining force of the instability. Currently, experimental and computational results exist for secondary droplet breakup caused by steady aerodynamic flows. However neither experimental nor computational results exist for droplets broken up by high frequency periodic flows. This study utilized a computational fluid dynamics program called STAR-CCM+ to model secondary droplet breakup in a periodic flow. By incorporating the volume of fluid multiphase flow model and varying boundary conditions, the behavior of the droplet in a sinusoidal flow was simulated at different ratios of the drop's natural frequency to the flow's oscillation frequency. This investigation tested predictions of the droplet response at different flow frequencies and made conclusions about fundamental droplet behavior.
Key words: combustion instability, secondary droplet breakup, CFD, multiphase flow

1. Introduction

Fluid mechanics is overall a very extensive research field, of which there still remains much to explore. Along with thermodynamics and chemistry, fluid mechanics plays a large role in the field of combustion. In the case of combustion in engines, such as liquid fueled rocket motors, there is a level of combustion instability that is reached during virtually every new technology development program. Typically a significant amount of time and money is invested into preventing these unstable combustor conditions, leading to a need for further research. Combustion instability is an area of research that is not fully understood and continues to challenge the development of future technologies.

Further, several studies have been performed in order to better understand secondary droplet breakup and results have proven very limited. In regards to experiments, many tests have been limited by materials and natural constants, such as gravity. With the increasing abilities of computational fluid dynamics, researchers have created limited simulations to model the multiphase steady flow situations.

1.1 Motivation

Overall, the importance of understanding secondary droplet breakup lies in the design and development of combustor technology that is more lightweight and operates with higher performance. Also, with increasing regulations and guidelines in the field of transportation engines, it is important to fill in the gaps where there is knowledge lacking within the fluid dynamics community. The applications of these important technologies are dependent upon fundamental knowledge of combustion instability and secondary droplet breakup. With further knowledge of these topics, there can be improvements in combustor design in terms of performance and fuel efficiency.

1.1.1 combustion instability

Combustion instability is characterized by periodic fluctuations during the combustion process and can be broken into three categories: low frequency (chug), intermediate frequency (buzz), and high frequency (screeching).[1] Each type of instability during combustion is undesirable. Instabilities can cause reductions in engine performance and potential damage to engine components due to increased heat transfer or system vibrations. Combustion instability is especially relevant to the design of more fuel efficient gas turbine and jet engines, which is crucial to the country's energy future. In order to increase fuel efficiency and decrease pollution, many jet engines are beginning to run on low fuel to air mixture ratios, also known as "fuel lean". This specific lean burn tends to cause more combustion instabilities due to more fluctuation and poses a challenge for current development of the technology.

Combustion instability may be caused by changes in drop size distribution, called secondary droplet breakup. Secondary droplet breakup is the splitting of large drops of injected fuel into smaller drops, which can occur within a series of regimes. During unstable combustion, the inconsistency in pressure can cause secondary breakup of large drops of fuel. In this case, the smaller drops are consumed more rapidly and the increased energy release with the addition of periodic flow, sometimes in the form of sound waves, can act as a sustaining force of the instability.

1.1.2 secondary droplet breakup

Secondary droplet breakup is defined as the splitting of large drops of liquid into smaller drops. Applications of this term can be found in liquid fueled spray combustion, raindrop formation, and in many other areas. Most commonly, droplet breakup has been found to depend on Reynolds number (Re) and Weber Number (We), both dimensionless parameters. Reynolds number, given by Equation 1, is the ratio of inertial forces over viscous forces while the Weber number, given by Equation 2, is the ratio of the continuous phase inertial force to the surface tension force. Weber number, through experimentation, has been determined as the most important

parameter for determining the timing of droplet breakup and the breakup characteristics. Equations 1 and 2 are as follows:

$$Re = \frac{\rho v d}{\mu} \tag{1}$$

$$We = \frac{\rho d v^2}{\sigma} \tag{2}$$

where, ρ is the density of the flow fluid, v is the velocity of the flow, d is the diameter of the droplet, μ is the viscosity of the droplet fluid, and σ is the surface tension between the two fluids.

The different regimes of breakup that exist include levels from vibrational to explosive, as shown in Figure 1. The most commonly reported regime is bag breakup, which is characterized by the drop initially flattening into a disk, with the center becoming thinner until it eventually bursts and forms small droplets. With experimentation, it has been determined that the boundaries between the regimes are not distinct and rather fading transitions.

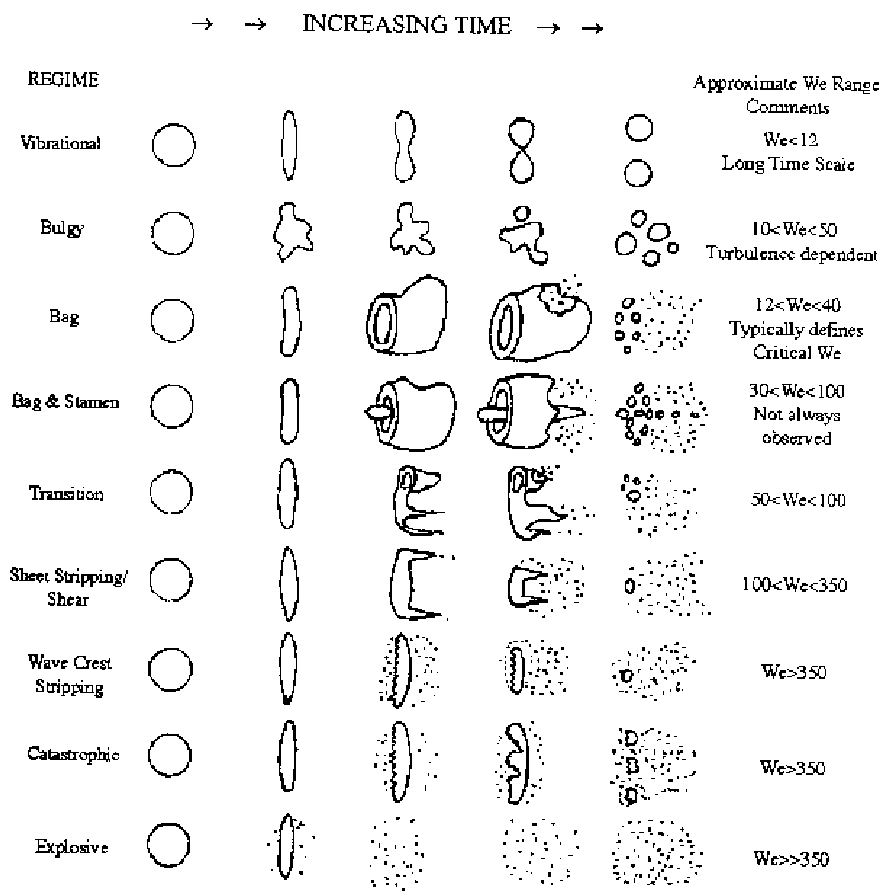

Figure 1. Regimes of Droplet Breakup[1]

1.2 previous studies

Currently, the majority of experimental and computational results regarding secondary droplet breakup exist based on the effects of steady aerodynamic flow; however, some studies of periodic flows do exist. The study "Secondary Droplet Breakup in Periodic Aerodynamic Flows”[1], describes the experimental results and predictions of the problem at hand. The study focused on the breakup at different frequency ratios, fa/fn, which is given as the acoustic frequency over the natural frequency of the droplet. The experiments, however, were limited by hardware to breakup results at a frequency ratio below 0.3, leaving the higher frequency range, especially that above 1, not understood. In this study, Bruno created an overall flow system with an acoustic generator attached that was built to simulate the reaction of drops in an acoustic flow field. With the use of a specifically designed drop generator, drops of test “fuels” of a controllable and repeatable size were subjected to flows of varying acoustic frequencies. Other limitations of these experiments included the imperfectly sinusoidal acoustic fluctuations and the free acceleration of the drops. In this study, Bruno also describes the Taylor Analogy Breakup Model, which is limited by the assumptions that the numerical constants are based on an arbitrary breakup condition and that breakup behaves like a linear spring-mass damper system. Using a FORTRAN code, the TAB model gave insight to how a drop may breakup in a sinusoidal load with the study of gradually applied loads. The current study was highly motivated by this study by Bruno and will seek to create reasonable simulations at the high frequency ratio conditions that could not previously be reached.

Han and Tryggvason studied the “Secondary Breakup of Axisymmetric Liquid Drops” in two parts: with acceleration by a constant body force[2] (1999) and with impulsive acceleration[3] (2001). In the first of the two part study, drop breakup was examined for small density differences between the drops and the surrounding fluid. A finite difference front-tracking numerical technique was used to solve the Navier-Stokes equations in this study. It was found that breakup is controlled by Eötvös number (Eo), Ohnesorge number (Oh), and viscosity and density ratios of the fluids. The study successfully ran axisymmetric simulations, in order to decrease run time, but still left a range of density ratios unstudied. In the second part of the study, Han and Tryggvason studied simulations of liquid droplets accelerated by a shock wave. The study examined the effect of We and density ratio on the breakup of drops in this impulsive flow situation and found that the computational results were consistent with similar experimental observations. Overall, these studies demonstrate that computational methods have been determined to effectively study types of droplet breakup, however there are many limitations to these methods that still exist.

According to a study by Cheng and Farmer[4], in 2005 no technique existed to accurately measure the flow field of dense spray combustion. Through computer simulations using the FDNS CFD code, Cheng and Farmer improved the computational efficiency of predicting thermal properties of real fluid models. By utilizing the linearized real-fluid model (LRFM), the study proposed an efficient approach for liquid spray flow simulation.

The importance of this study lies in the "proof of concept" that current computational methods are capable of such simulations.

Another "proof of concept" study is that of Lin et al.[5], which studied the CFD capabilities of modeling multiphase flow. This study noted the use of the Volume of Fluid (VOF) model, described later in this paper, as the best model for stratified and slug internal flow through a pipe. Although this study was fundamentally different in flow type than the current study, it is important due to the lessons learned for studying multiphase flow. The study found that the advantages of the model are the predictions of stream wise flow velocities and flow patterns. It is noted, however, that one must be wary of the accuracy of each multiphase model and that the model provided an inaccurate prediction of a liquid-vapor wavy interface with large velocity differences. The study also makes note of the importance of a good quality mesh to the accuracy of CFD simulations, which is taken into account in the current study.

With the effects of high frequency sinusoidal flows on secondary droplet breakup poorly understood, the current computational capacities of Computational Fluid Dynamics were tested with a task of this caliber. With such an increase in CFD capabilities, it is important to utilize the resources available and solve a problem that is fundamental to the fluid dynamics research community.

2. Objectives

The goal of this project was to determine if the effect of a perturbed flow on droplet breakup is significantly different than the effect of a steady flow. Also, this study determined the effectiveness of current CFD codes in studying this problem. A focus was placed on simulating a periodic flow around a droplet of fuel in a computational fluid dynamics interface and comparing the results with known computational simulation results and experimental data of similar situations with a steady flow.

The scope of the project was to increase the fundamental knowledge about droplet breakup in an area that has not been heavily researched to date. With current computational power, it is now possible to represent complicated fluid dynamics situations on a computer for which experiments are not possible. This project focused on comparing computational data using a droplet in steady flow to experimental results andpreparing several cases of a periodic flow for the same droplet. This included the preliminary study of a solid sphere in a steady flow, a deformable sphere in a steady flow, and the final tests of a deformable sphere in a periodic flow.

3. Methodology

3.1 resources

In order to complete the stated objectives, the approach of this research project is a computational method using a CFD program called STAR CCM+ (standing for computational continuum mechanics). No equipment is

necessary beyond the licenses to the CFD program and the availability of the Union College Mechanical Engineering Department computer labs.

3.1.1 budget

For the completion of this project, the National Science Foundation Scholars Program granted a fund of $1000. Due to the minimal resources necessary for the project, the budget is currently being saved for the potential to be used to present this research at an engineering conference.

3.2 verification case

In order to prove the effectiveness of the computational program and chosen models, a verification case was run before any simulations were created. This verification case aided during the instructional period of the project and assisted in developing a methodology for future simulations. The results of this case were compared to ensure that the methodology was reasonable.

3.2.1 geometry

To begin a simulation, STAR CCM+ requires a geometry file to be imported. To simulate a solid sphere in a wind tunnel, a spherical curve was removed from a large piece of material. The fluid, which is the air represented by the material shown in the geometry, was modeled as a cylinder oriented horizontally with a radius of 0.152 m and a length of 0.914 m. The spherical cut-out is located in the center of the cylinder and has a radius of 0.0127 m. In order to take advantage of the symmetry plane boundary conditions that are available in STAR CCM+, the geometry model was created as a quarter portion of a full cylinder wind tunnel section. It should be noted that in order to minimize the effects of the outer wall of the model, the entire geometry created is quite large when compared to the solid sphere cutout alone. A screenshot of the described model is shown in Figure 2.

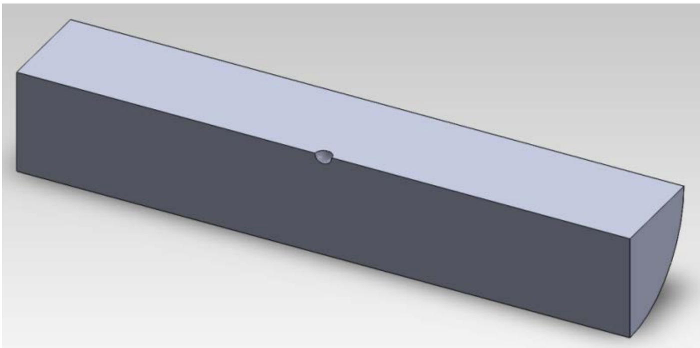

Figure 2. Screenshot of the Verification Case Geometry in SolidWorks

3.2.2 boundary conditions

When imported into the program, the geometry began as a single region. The verification case model includes six different boundaries that were split from the entire region by an angle of 45 degrees. This allowed for each of the sharp edges to be considered the separation points between the required boundaries. The boundaries include a velocity inlet on the left side of the cylinder and a pressure outlet on the right side of the cylinder. The top and front boundaries shown in Figure 2 are represented as symmetry planes to simulate a full cylindrical model. The last two boundaries are that of the curved sphere cutout and that of the curved outside surface, which are both modeled as walls. By modeling these boundaries as walls, a no slip condition was employed and an impermeable surface was modeled, creating a separation between the fluid and the solid bodies. The differentiation of the boundaries affects the slip conditions and how the fluid, or air, is simulated to flow through the geometry.

3.2.3 meshing

A major portion of a computational model is the creation of a well-refined mesh. A mesh is a collection of cells for which calculations are performed computationally to arrive at a final solution. It is important that a mesh is well refined in order to allow for an accurate solution.

When the initial mesh is imported, the surface must be remeshed through meshing model selection and using surface and volume meshers. For the verification case, the selected meshing models included the “Surface Remesher”, the “Prism Layer Mesher”, and the “Polyhedral Mesher”, with all settings remaining at the default values. The wall boundary between the sphere and the fluid was defined as the feature curve, which employs a more refined mesh in this area. The reference values, including base size, surface growth rate, and surface size, were altered in several iterations to arrive at a successful mesh. The surface mesh that was created can be seen in Figure 3. The cells in this mesh only apply to the surface and are shaped as triangles. The surface growth from the defined feature curve around the sphere can be visualized in this screenshot.

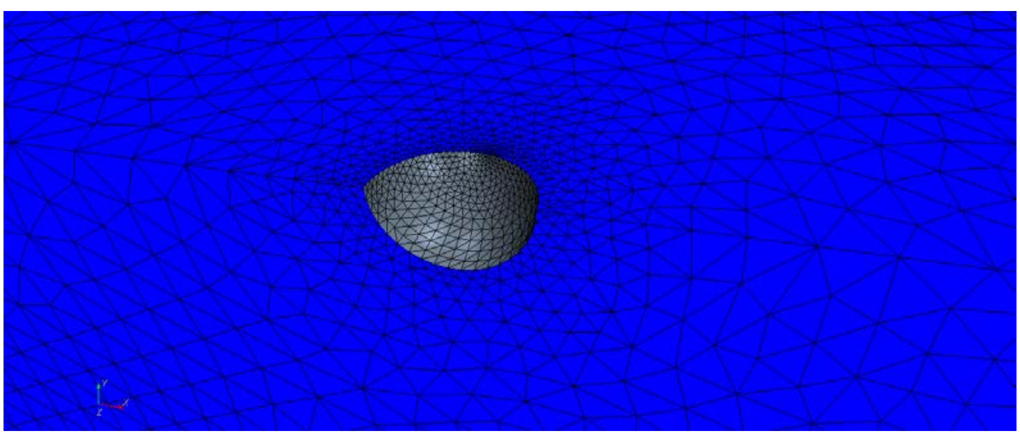

Figure 3. Surface Mesh of the Verification Case

After the surface mesh was complete, the volume mesh was created. This mesh features cells that are polyhedral shaped and cover the entire volume of the geometry. It should be noted that creating the volume mesh is significantly more time consuming than creating the surface mesh. The representation of the volume mesh can be viewed as an entire geometry in Figure 4 and as a close-up of the feature curve in Figure 5.

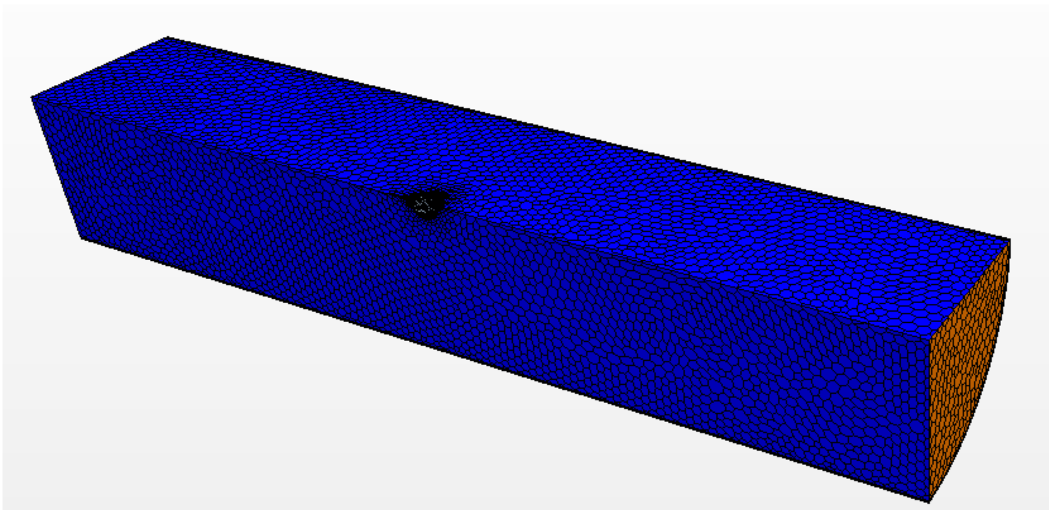

Figure 4. Volume Mesh of the Given Verification Case Geometry

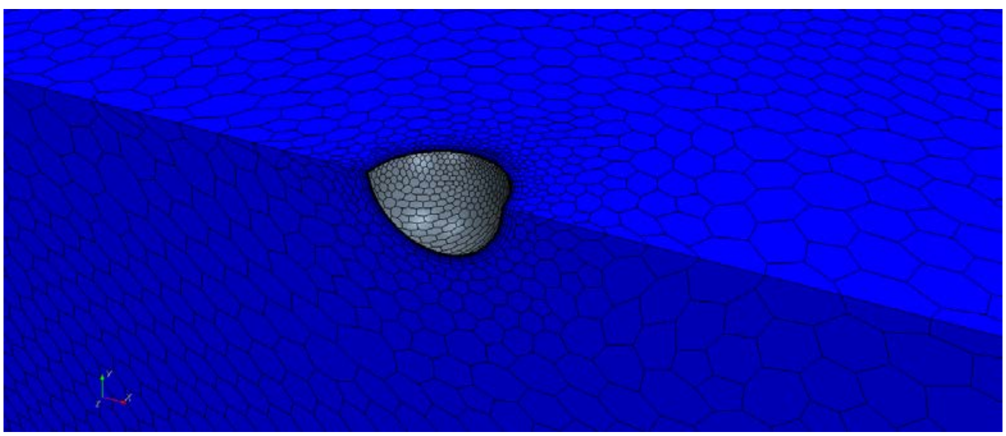

Figure 5. Feature Curve of the Volume Mesh

The mesh, as displayed in Figure 4, includes a total of about 700,000 faces. The base size was set to 1.0 m and the relative minimum and target surface sizes were set to 0.01% and 1000% of the base size, respectively. The number of prism layers was set to 10, the prism layer stretching was set to 1.5 and the relative size of the prism layers was set at 200% of the base size. In order to further refine the sphere, the curvature setting of number of points per circle was set to 72. The surface growth rate, or the rate of increasing polyhedral side lengths, was set to 1.3. Finally, the Tet/Poly density was set to 5, with a growth factor of 0.1.

3.2.4 physical models

Before a simulation can be run, it is necessary to accurately choose the physical models that will be utilized. The original validation case simulation included the choice of both the 3-Dimensional and Steady physical models. The fluid was also modeled as laminar and a situational Re was calculated at approximately 25000. The fluid in the wind tunnel, modeled as a constant density gas and given the properties of air, was also modeled as coupled flow. There is a choice that exists between coupled flow and segregated flow that is dependent upon the simulation. Coupled flow is appropriate for all compressible flows and requires more memory than the segregated flow model. The coupled flow model was chosen in this simulation because it tends to promote accuracy and is recommended if computer resources are not an issue.

3.2.5 results

The simulation was completed using the computational model of a solid sphere in a steady flow. The model was run for 1000 iterations and the residuals are shown in Figure 6.

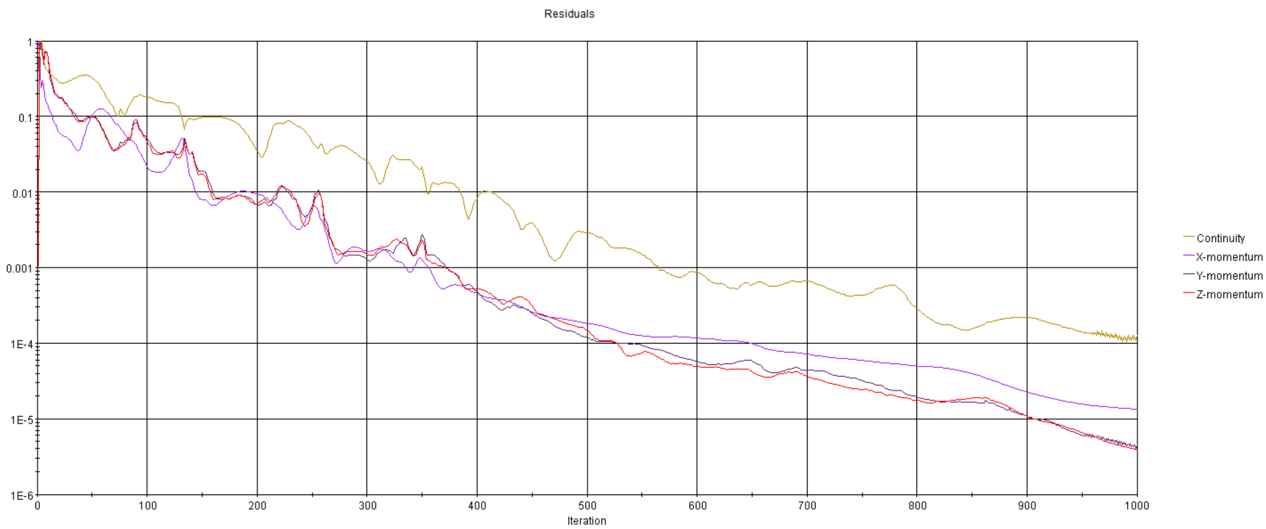

Figure 6. Graph of the Residuals for the Solid Sphere in Steady Flow Simulation

For this simulation, a vector scene was created to represent the velocity flow field around the sphere. This vector scene is shown in Figure 7. As shown in this scene, there is an increased velocity around outside of the sphere, a zero velocity stagnation point at the front of the sphere, and a small low-velocity wake following the shape. A corresponding scalar plot of the velocity is also shown in Figure 8.

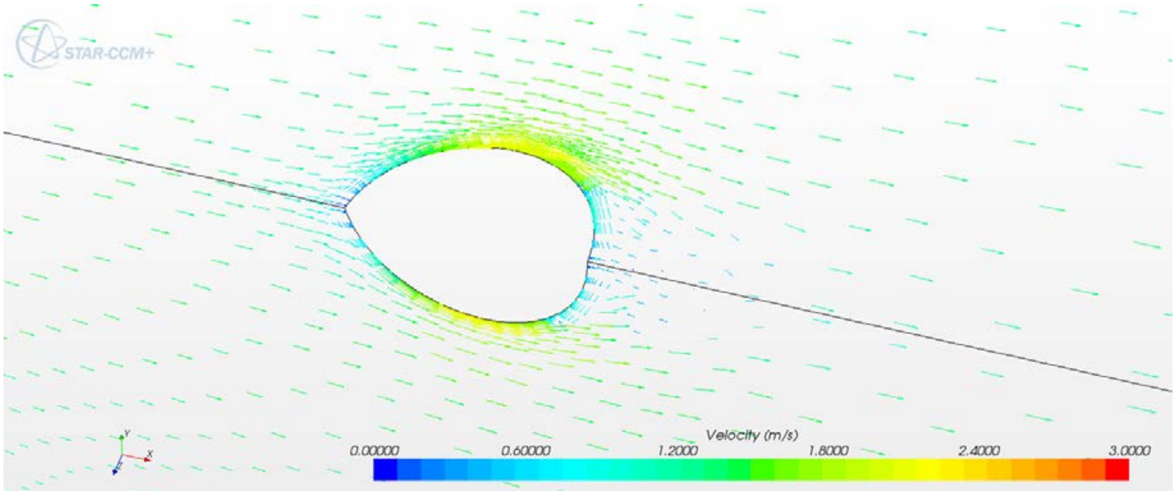

Figure 7. Vector Scene of the Velocity Flow Field around the Solid Sphere

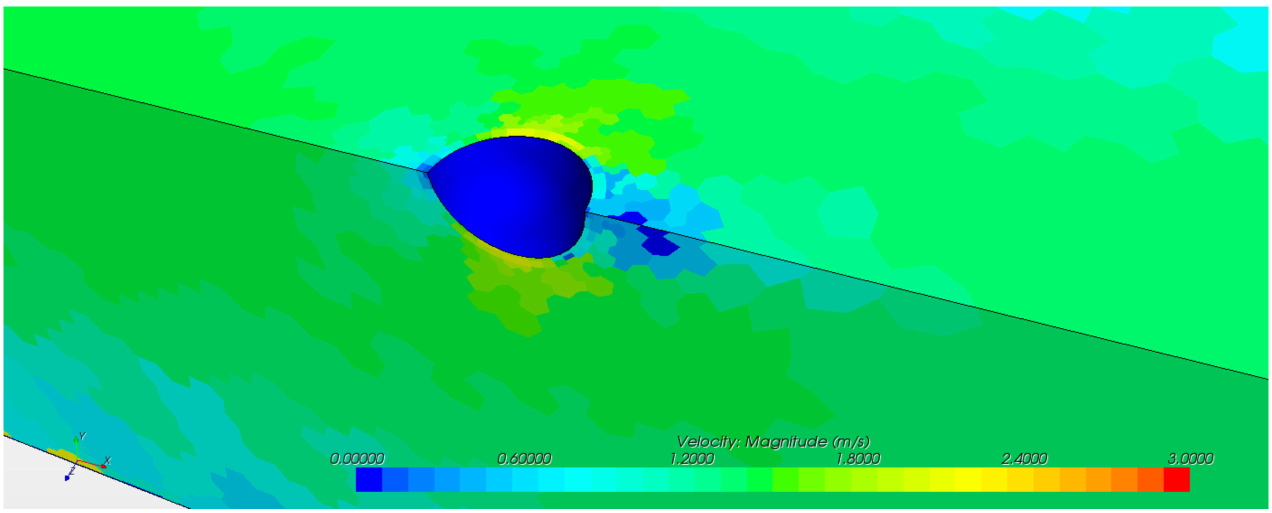

Figure 8. Scalar Scene of the Velocity Values around the Solid Sphere

This simulation also included a scalar plot of the pressure distribution along the solid sphere, which is shown in Figure 9. The results of this pressure distribution showed an area of low pressure around the outside curvature of the sphere and an area of high pressure where the airflow makes initial contact with the sphere.

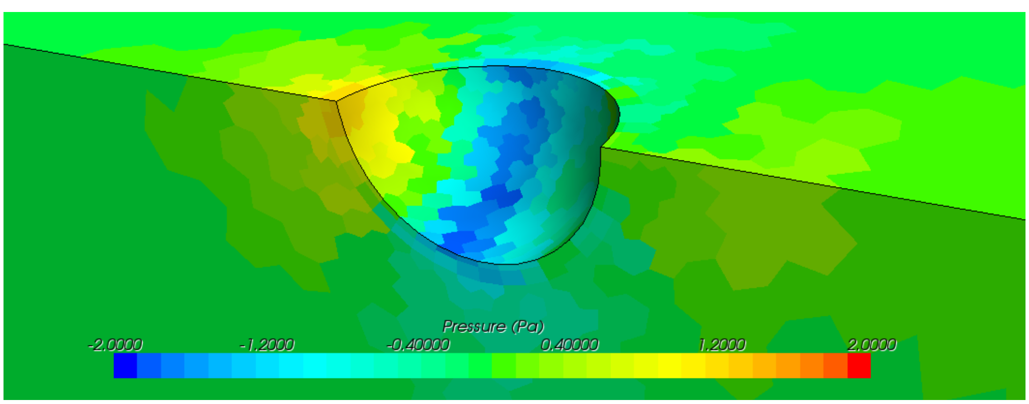

Figure 9. Pressure Distribution along the Solid Sphere

3.2.5 comparison to known results

Based upon the known response of a spherical object in a steady flow, the results of the verification case show a positive qualitative agreement. Shown in Figure 1 in Attachment A are the laminar vs. turbulent trends for flows over a cylinder, a similar case, at different Reynolds numbers. Even with a coarse mesh, Figure 8 shows the clear stagnation point at the front of the droplet and wake at the back, both in shades of blue. There is also an increased velocity around the center axis of the droplet, as expected. Figure 9 shows a high pressure area at the stagnation point followed by low pressure around the center of the droplet, also as expected. With a qualitative match, it is evident that the physical situation that was modeled in the verification case is accurate.

4. Computational Model

A final computational model was created and tested for use with steady flow and periodic flow simulations. The geometry, meshing, and physical model choices are outlined in more detail in this section.

4.1 Geometry

For the computation, a SolidWorks file was created of the appropriate geometry and saved as an .STL file so that it could be imported as a surface mesh into STAR CCM+. Similar to the verification case, the geometry was modeled as a quarter cylinder piece with a length of 1 m and a radius of 0.25 m. Unlike in the verification case (section 3.2 above), this model did not include a spherical cutout to represent a solid object in the center, as the water and air are both modeled as fluids. A screenshot of the geometry can be found in Figure 10.

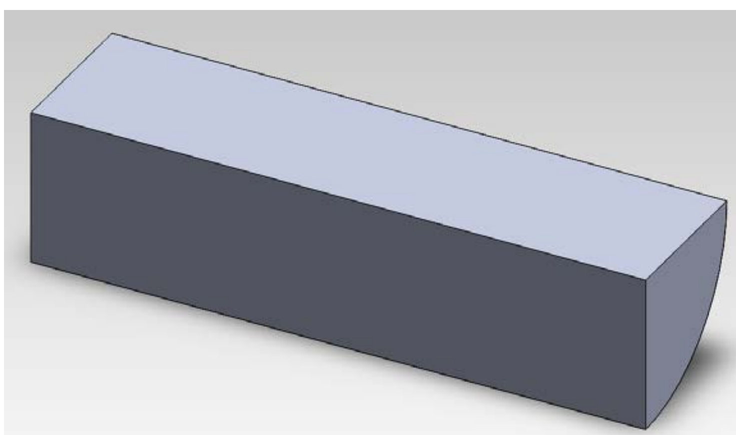

Figure 10. Computational Model Geometry in SolidWorks

4.1.1 boundary conditions

The geometry, when imported into STAR CCM+ as a surface mesh, was split from a single region into five boundaries by an angle of 45 degrees. The boundaries were labeled as a velocity inlet on the left side of the

cylinder, a pressure outlet on the right side of the cylinder, symmetry planes on both the top and front boundaries of the cylinder, and a wall on the outside curvature of the model.

4.1.2 orientation

For later steps during the meshing and simulation, it was important to reorient the model based upon a laboratory coordinate system. Region 1 was transformed first by scaling of a uniform 0.001 value, in order to relate the model lengths directly to the given geometry length. The model was also translated and rotated until the axis was located on the corner of the symmetry planes and the inlet, as shown in Figure 11. Finally, a translation in the positive x-direction at a value of 0.001 is necessary to allow for the axisymmetric model to be chosen. Without this small translation, an error stating that all values must be at or above the axis of rotation, or the x-axis, will occur.

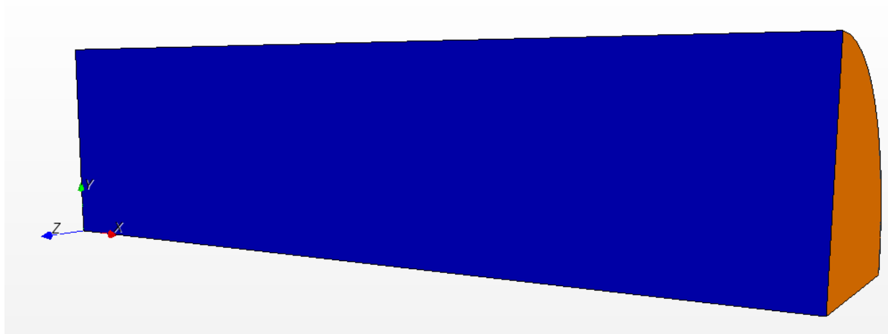

Figure 11. Appropriate Orientation of the Geometry

4.2 Meshing

For the production of a reliable simulation, it was important to assign a well-refined mesh to the geometry. The "Surface Remesher", "Polyhedral Mesher", and "Prism Layer Mesher" were each chosen for the model. For these meshing models, the base size was set to 0.001 m, the prism layer thickness was assigned to 100%, the relative minimum surface size was set to 100%, and the relative target surface size was set to 500%, with all percentages relative to the base size. All other meshing values were left at the defaults.

In order to create a well-refined area near the drop location in the center of the geometry, it was necessary to employ a volumetric control. A new volume shape was created from tools and a sphere was "snapped to the part" with an origin of [0.5,0,0] and a radius of 0.025 m. Then a new volumetric control in the meshing models was created using the new sphere. Each check box to customize the three meshing models was selected for the volumetric control and the custom size was changed to 20% of the base size. This custom size generated considerably smaller grid size around the spherical shape in the center of the geometry. A surface mesh and a volume mesh were both generated using these values.

To shorten the overall simulation time, the 3D volumetric mesh was converted into a 2D axisymmetric mesh. With this action the regions and continua relating to the 3D model were deleted. The 2D mesh can be seen in both Figure 12 and Figure 13.

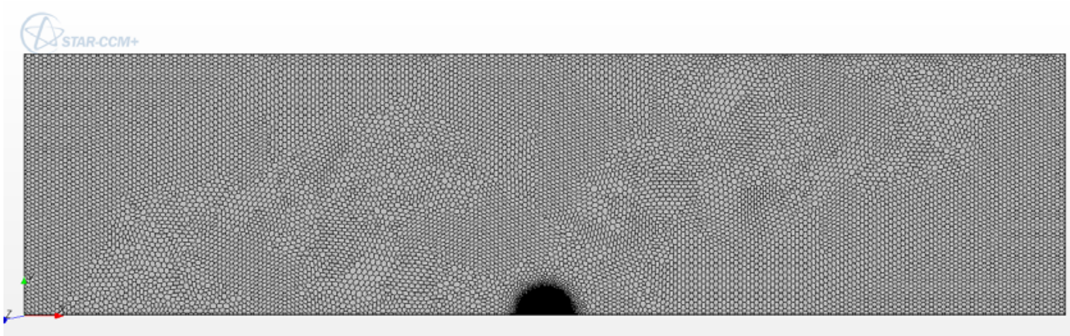

Figure 12. 2D Mesh of the Computational Model

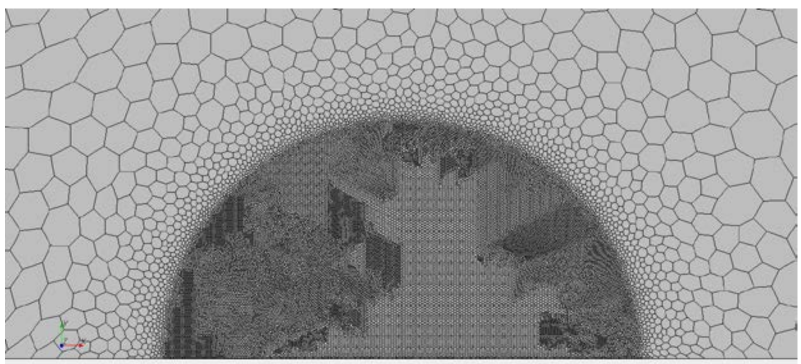

Figure 13. Close-up View of the 2D Mesh

4.3 Physical Models

For the purpose of accurately modeling a water droplet in a wind tunnel, several physical models were chosen. With the use of a 2D mesh, the "Axisymmetric" model was selected, with the x-axis as the axis of symmetry. This allowed, again, a reduction in simulation time, by cutting down the model number of nodes. With a non-spherical initial droplet, this case would not be applicable. Also any non-axisymmetric effects are lost from the simulation. The "Implicit Unsteady" model was chosen based upon the unsteady nature of the breakup situation. The "Multiphase Mixture" model, followed by the "Volume of Fluid" model, was chosen in order to allow a separation between water and air to be defined. The "Segregated Flow" model was chosen rather than the "Coupled Flow" model based upon limited computational capabilities and compressibility of the flow. The Reynolds number for the various flow velocities was calculated to range from 6330 to 53800, allowing the laminar physical model to be chosen. As shown by the graph in Figure 2 in Attachment A, the maximum Reynolds number in the calculated range is approaching turbulent flow; however, this high velocity case was modeled as laminar. "Surface Tension", which is a very important aspect of droplet-air interaction, was chosen

from the optional models along with the segregated fluid isothermal model. It is also important to note that the "Gravity" model was not chosen for this simulation, in order to restrict the forces on the droplet to just one coordinate direction, the x-direction. The y-component of the physical force on the droplet is simple to remove in a computational simulation, but would be inevitable in an experimental situation. With each of these chosen, the physical situation of the model was established.

To create the desired fluid situation, two new Eulerian phases were created under the "Eulerian Multiphase" tab. It is important that water was created first, modeled as a constant density liquid, and air was created second, modeled as an ideal gas. All of the default values for water and air given by STAR CCM+ were left unchanged. Under the physics initial conditions, the constant pressure was left at 0 Pa, the static temperature was left at 300 K and the constant velocity was kept at 0 m/s. Under the volume fraction initial condition, the method was changed to composite, as a combination of water first and air second. In order to define the size and location of the water droplet, a field function was created from the tools menu. The function, labeled 'drop', was created using the coding method of STAR CCM+. The 'drop' code is read as follows:

```
($$Centroid[1]<=(sqrt(0.0001-pow(($$Centroid[0]-0.5),2))))&&($$Position[1]>0)?1:0
```

The code utilizes the known functions of Centroid and Position, as well as the coordinates of [0,1,2] equating [x,y,z]. The code also uses the equation of a circle to define the location of the water. Verbally, the code reads: if the y value of the geometry is less than or equal to $\sqrt{0.0001-(x-0.5)^2}$ and the position is above the x-axis, then the value is 1, else the value is zero. When placed as the field function value for the volume fraction of water, this states that water exists within the two defined boundaries, when the value is 1. The volume fraction initial condition of air was left at 0, and therefore it was assumed that air was located in all areas not defined as water. Also, the surface tension between the water and air was left at a standard default value of 0.074 N/m.

3.4.1 volume of fluid model

The volume of fluid (VOF) physics model is a simple multiphase model that is often used to simulate two-fluid flows. The basic equations of the model, as given by the STAR CCM+ Training Guide, can be found in Attachment B. The model is well suited for flows where each phase is a large structure and there is small contact area between phases. For example, the VOF model is better suited for a single droplet in steady flow as compared to many droplets in steady flow, which proves the applicability for the current study. It is noted, however, that water droplets in air require a mesh of at least three cells across each droplet in order to produce a reasonable result.

In this model, the value C is used to represent the fraction of the reference phase that is present in each grid cell, called the volume fraction. The value of C can vary from 0 to 1 in empty and full cells, respectively. The

model proceeds by reconstructing the shape of the fluid interface and determining the amount of reference phase volume that is exchanged across the boundaries of neighboring cells. The volume of fluid model works by advecting a marker function to identify fluids, and the boundaries between them, directly.

3.4.2 solvers and stopping time

Solvers are an important aspect of simulations, which can cause large changes in simulation results with only small changes in values. For the implicit unsteady solver, a time step of 0.001seconds was chosen for all of the simulations. Also, 2nd-order temporal discretization was used, in order to help control the diffusion of the water droplet. For the segregated VOF solver, the under-relaxation factor was changed from 0.9 to 0.5. Changing this value was able to help with convergence and overall accuracy of the model.

In regards to stopping criteria for the model, the number of inner iterations was left at the default value of 20. The inner iterations determine how many iterations will be completed during each time step. To determine the effect of the inner iterations on the computational model, test cases were run by changing only that variable, as shown in Figure 14 through Figure 17.

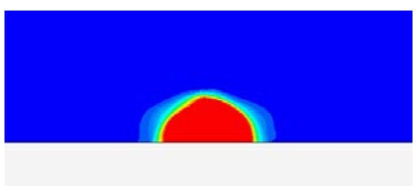

Figure 14. Water Droplet with Zero Flow after 0.1 s

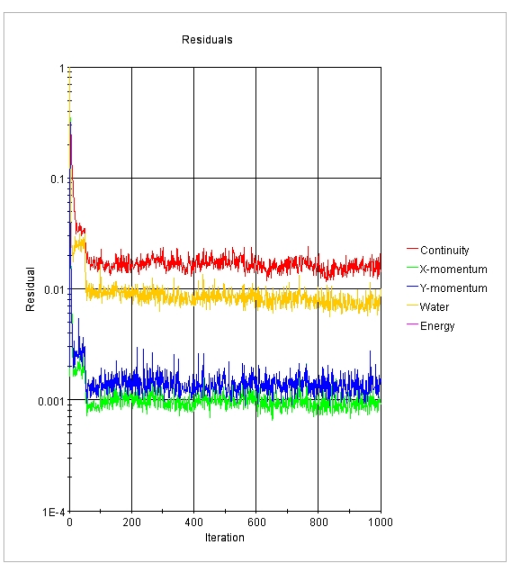

Figure 15. Residuals from the Simulation Shown in Figure 14

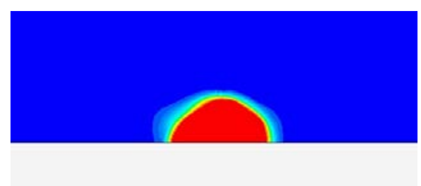

Figure 16. Water Droplet with Zero Flow after 0.1s

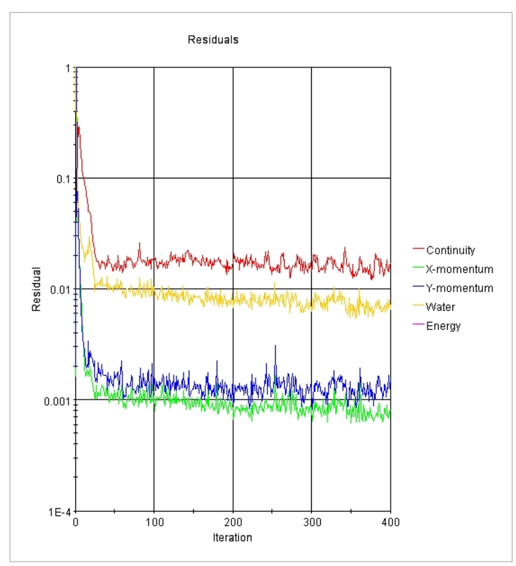

Figure 17. Residuals from the Simulation Shown in Figure 16

Both water droplets were simulated for the same amount of physical time with a different number of iterations. When the results are compared there is not a significant difference in either the diffusion or the residuals to

warrant the extended simulation time necessary for more inner iterations to be used. The maximum physical time was changed depending on each individual simulation and the maximum steps option was deselected for all simulations.

During each solution, it was also important to be aware of the trend of the residuals. In a reliable simulation, the residuals decrease and level off to a low value, usually below 0.01 in these cases. For some simulations, depending on the flow situation, the residuals had a significant amount of oscillation, which could equate to a less reliable result.

3.4.3 scenes

As a way to view the model during simulations, two different scalar scenes were created. A scalar scene for both velocity and the volume fraction of water exist for each simulation. For these scenes, the update policy was assigned by time-step and an annotation was added to print the physical solution time on the screen. Also, the scalar field of the variable color bar was changed according to the minimum and maximum values of each simulation and the automatic update option was deselected to keep the color scale the same as the simulations were completed. The scenes were saved to files as .jpg and used to view and compare the simulation results.

5. Results

As a validation of the model, both the zero flow case and steady flow cases at various Weber numbers were completed. The cases were refined to follow known results and physical trends of droplet breakup. Once the cases were compared and validated, preparations for periodic flow cases at various Weber numbers and frequencies were completed.

5.1 Zero Flow

As a test, a case with a We = 0, or zero velocity, was simulated using the current computational model. In this case, run for 0.25 s, the droplet was expected to show no movement or changes in shape. Originally, this case experienced some unphysical deformation, creating bumps at the interface between the droplet and the air. This was corrected with a reduction in time step from 0.005 to 0.001 s and a change in the VOF under-relaxation factor. As shown in Figure 18, the final results show the expected behavior, with only a small amount of (undesirable) numerical diffusion at the interface between the water and air. If run for a longer period of time, this diffusion is likely to increase. For the purposes of this study, however, the results produce a sufficient level of qualitative agreement with the known physical case.

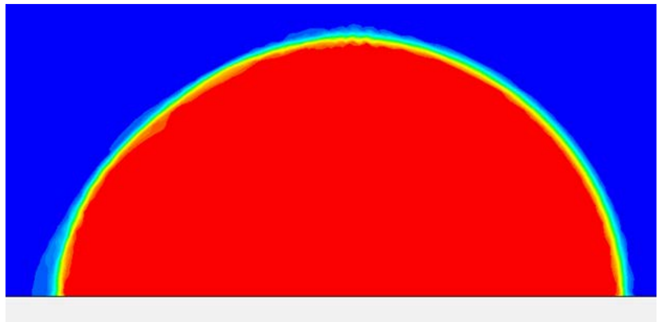

Figure 18. Volume Fraction of Water at t=0.25 s for a Zero Velocity Case

5.2 Steady Flow

As easily comparable cases to known experimental results, steady flow cases at various Weber numbers were simulated. Although droplet breakup is a naturally transient process, the terminology “steady flow cases” refers to a simulation that is run using the “Implicit Unsteady” physical model. For each of these “steady flow cases” a constant velocity is provided at the inlet and remains unchanged throughout the simulation , thereby naming it steady. Weber numbers of 6, 12, 100 and 450 were chosen based upon the values given in Figure 1, in order to model vibrational, bag, shear, and catastrophic breakup, respectively. In order to vary the Weber number, the required inlet velocity was calculated and set for each case. Each case is shown below, in Figures 19 through 22, at various time steps to illustrate the sequence of breakup. As a result of choosing different time steps to demonstrate each simulation, the cases cannot be compared in vertical columns except for the initial point. It should be noted that when the drop begins to move in the positive x-direction with the flow it is eventually no longer located within the highly refined sub region of the mesh. That is the droplet advects into the coarse mesh region, and the simulation looses significant spatial resolution. The boundary between the highly refined and coarse mesh sections that are described is shown clearly in Figure 13, with the surface growth factor resulting in the rapidly changing grid size when moving from the center. The net effect of this change is that some of the later time steps in each simulation experience considerably more diffusion and sometimes unlikely shapes result. However, these simulations do demonstrate that as long as the mesh has sufficient spatial resolution the models chosen produce good qualitative agreement with droplet breakup behavior observed experimentally.

When compared to the diagrams of known breakup regimes in Figure 1, the simulations of the steady flow match the physical trends well. Figures 19 through 22 were created as a compilation of saved scene views that demonstrate the transitional shapes of the droplet during each simulation. Each simulation produced one scene file for each time step, which the views below were chosen from. Each of the simulations in Figures 19 through 22 was created using the volume fraction scale in Figure 23.

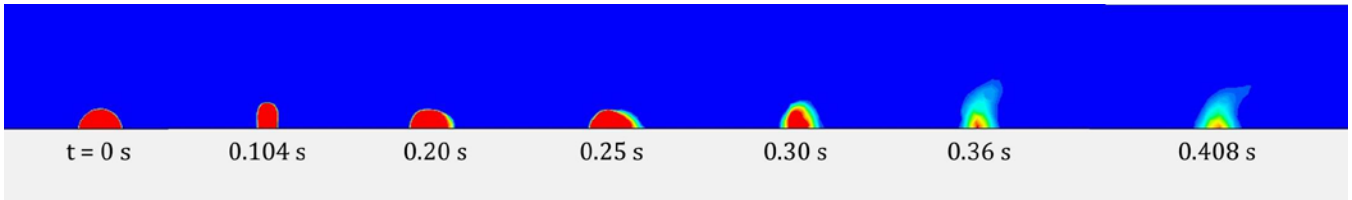

Figure 19. Steady Flow Case with We=6 and Vibrational Breakup

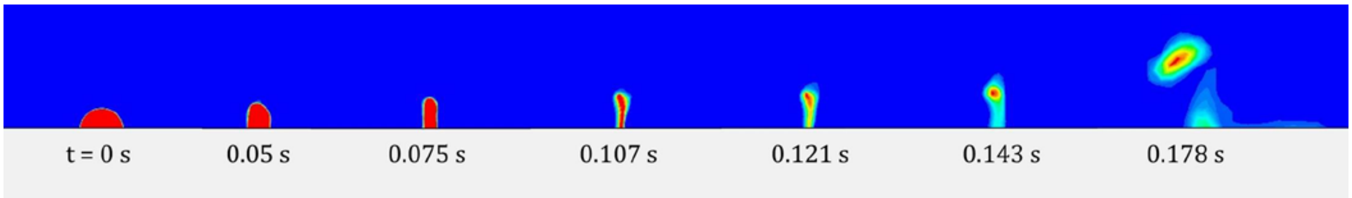

Figure 20. Steady Flow Case with We=12 and Bag Breakup

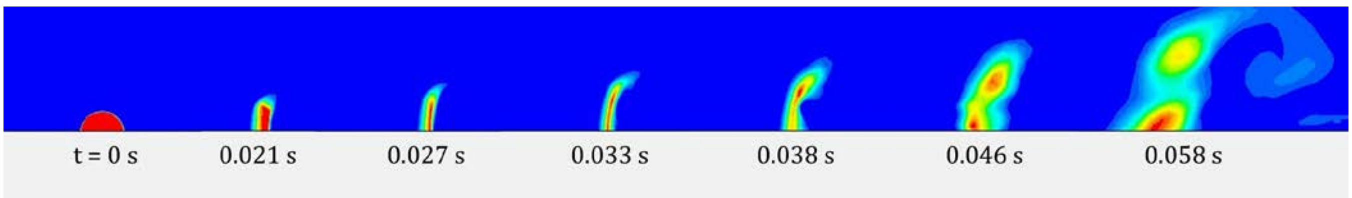

Figure 21. Steady Flow Case with We=100 and Shear Breakup

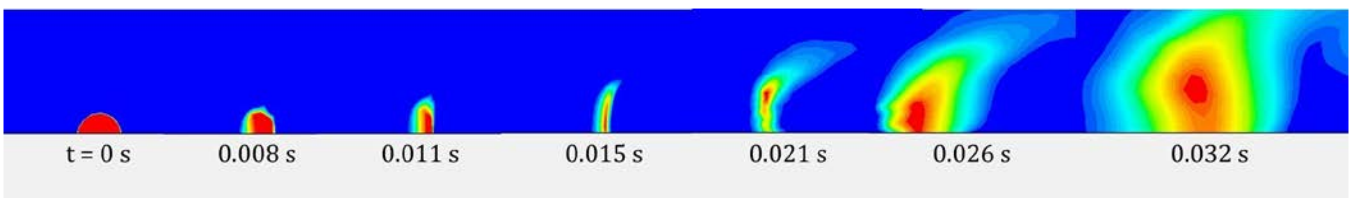

Figure 22. Steady Flow Case with We=450 and Catastrophic Breakup

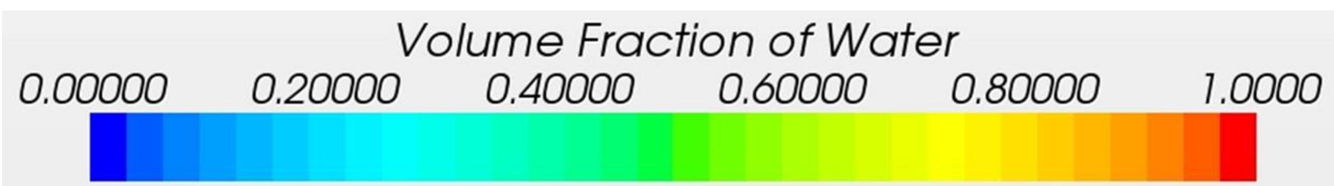

Figure 23. Volume Fraction of Water Scale for All Steady Simulations

5.3 Periodic Flow

Periodic flow cases, unlike the steady cases that were completed, are characterized by the droplet experiencing an oscillating, or sinusoidal, velocity. Every water droplet naturally oscillates with a period of oscillation given by Equation 3[1],

$$T_{NF} = 2\pi\sqrt{\frac{\rho_d d_d^3}{64\sigma}} \tag{3}$$

where ρ_d is the density of the droplet, d_d is the diameter of the droplet, and σ is the surface tension between the fluids. This oscillation period can be converted to a frequency and then to an angular frequency using both Equation 4 and Equation 5 in sequence.

$$f_n = \frac{1}{T_{NF}} \tag{4}$$

$$\omega = 2\pi f_n \tag{5}$$

For the droplet size created in this simulation, a natural frequency of 3.877 hz was calculated. The interest of this study lies in the effect of sinusoidal flows at different ratios of acoustic frequency to droplet natural frequency, given by f_a/f_n. In order to input the oscillating velocity as the inlet velocity, a field function was created from the tools menu. The function was created using the coding method of STAR CCM+ and is read as follows:

```
($Time>0)?[A*sin(ω*$Time+ϕ),0,0]:[0,0,0]
```

The code utilizes the known Time function, as well as the coordinates of [0,1,2] equating [x,y,z]. During a simulation, the amplitude, A, the angular frequency, ω, and the phase, ϕ, would be defined as numerical values to describe a Weber number, frequency ratio, and phase respectively. Verbally, the code reads: if the time is greater than zero, the x-value of the velocity is equal to Asin(ωt), else the velocity in all directions is zero. This code, once refined, will be used to study the periodic flow situation on the droplet using the computational model created.

5. Future Work

Next term, as time allows, corrections to current simulations and additions of new simulations will be made to improve the quality of this study.

First, corrections to the current steady flow cases will be made. Test cases will be run to qualitatively measure the effect of the “Sharpening Factor” as compared to the “Under-Relaxation Factor” on droplet diffusion, and changes to the model will be made accordingly. Also, the mesh may be refined further in the horizontal direction to allow a smaller chance that the spatial resolution of the simulation is lost due to mesh growth. Finally, a transitional Weber number value between each significant breakup regime will be determined specifically for this computational model. Although a general separation between breakup regimes is established in Figure 1, a different model can cause the already vague lines between regimes to shift slightly.

Once transitional Weber number values are determined, a series of simulations will be completed that model the periodic flow situation. There are four different variables that can be altered to change the flow situation for different simulation cases, namely amplitude, offset, frequency, and phase. Amplitude is determined by the desired weber number and is the maximum flow velocity magnitude that will be reached during a simulation. Offset, which will be disregarded in this study, is a locational value that changes where the sinusoidal wave axis is in comparison to the droplet location. This value has applications in an actual engine with the location of the acoustic waves in comparison to the fuel injection location. The frequency value will be altered to

change the ratio f_a/f_n. Special interest exists in the results for high frequency ratios, over 1, due to the strong lack of experimental results at these values. The phase, the last variable, is equivalent to the point along the sine wave that the droplet is exposed to first. This value affects whether the flow is accelerating or decelerating at initial contact, which could significantly alter the droplet response to the flow.

In order to implement the field function code for the sinusoidal flow properly, it must be determined through test cases whether STAR CCM+ expects a value in degrees or radians as the input to the sine function. With transitional Weber numbers between droplet breakup regimes determined, amplitude values will be chosen very carefully to control the Weber numbers. There are predictions that exist for high frequency oscillating flows that state if the frequency of the flow is much higher than the natural frequency of the droplet, the droplet will respond to the average velocity magnitude. In order to test this prediction, Weber numbers must be chosen very close to the breakup regime boundaries so that the average velocity magnitude creates a Weber number that is in a regime below that originally inputted.

Once simulations are produced for the different Weber number cases, a way to strengthen the case of the results is to demonstrate similar results for different Ohnesorge numbers. Ohnesorge number is a dimensionless number that relates the viscous force to inertial and surface tension forces and is given by Equation 6,

$$Oh = \frac{\mu}{\sqrt{\rho \sigma d_d}} \tag{6}$$

where μ is the viscosity of the liquid, ρ is the density of the liquid, σ is the surface tension, d_d is the diameter of the droplet. As shown on page 33 of *Secondary Droplet Breakup in Periodic Aerodynamic Flows*, there is a change in the relationship of Weber number to breakup regime as Ohnesorge number increases. The recreation of this figure using computer simulations as data points would further prove the validity of my model.

Overall, there are several tests and simulations that must be run to improve the current results and to create new results and fundamentally new knowledge in the world of secondary droplet breakup.

6. Acknowledgements

The funding for this project was provided by the Union College National Science Foundation Scholars Program. The author would also like to thank Rhonda Becker and Stan Gorski of the Mechanical Engineering department and fellow students Preston Thompson and Rebecca Slosberg.

In particular, the author would like to thank Professor Bruno for his knowledge, support, and encouragement throughout the project.

7. References

1. Bruno, Bradford A. *Secondary Droplet Breakup in Periodic Aerodynamic Flows.*Ph.D. dissertation, Pennsylvania State University, 2000.
2. Han, Jaehoon, and GretarTryggvason.“Secondary Droplet Breakup of Axisymmetric Liquid Drops.I. Acceleration by a Constant Body Force”.*Physics of Fluids* 11.12 (1999): 3650-667.
3. Han, Jaehoon, and GretarTryggvason. “Secondary Droplet Breakup of Axisymmetric Liquid Drops.II. Impulsive Acceleration”.*Physics of Fluids* 13.6 (2001): 1554-65.
4. Cheng, G. C., and R. C. Farmer. "Numerical Simulation of Spray Combustion Flows with a Linearized Real-fluid Model." *Computational Methods in Multiphase Flow III* 50 (2005): 193-206.
5. Lin, D, P Diwakar, V Mehrotra, B Rosendall, and J Berkoe. "Modeling Multi-phase Flow Using CFD with Related Applications." *Computational Methods in Multiphase Flow III* 50 (2005): 251-61.
6. Tryggvason, Grétar, Ruben Scardovelli, and StéphaneZaleski. *Direct Numerical Simulations of Gas-liquid Multiphase Flows*. Cambridge: Cambridge UP, 2011.
7. STAR CCM+, *Training Guide*
8. Bensen, Tom. "Drag of a Sphere." National Aeronautics and Space Administration, 16 Sept. 2010. Web. <http://www.grc.nasa.gov/WWW/k-12/airplane/dragsphere.html>.

Attachment A.[8]

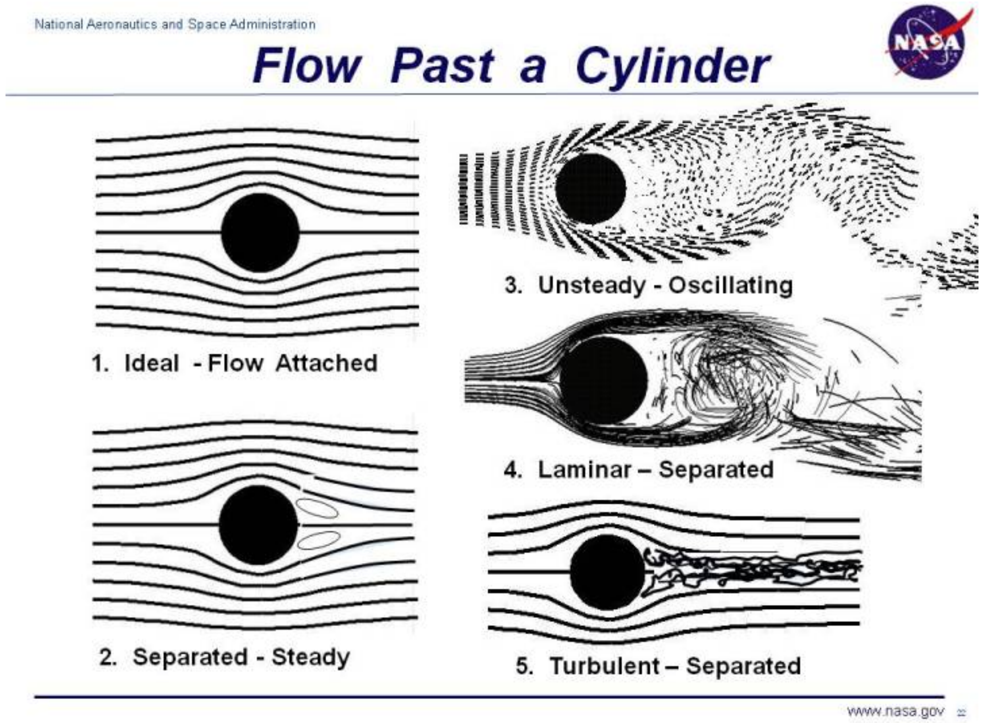

Figure 1. Flow Types Over a Cylinder

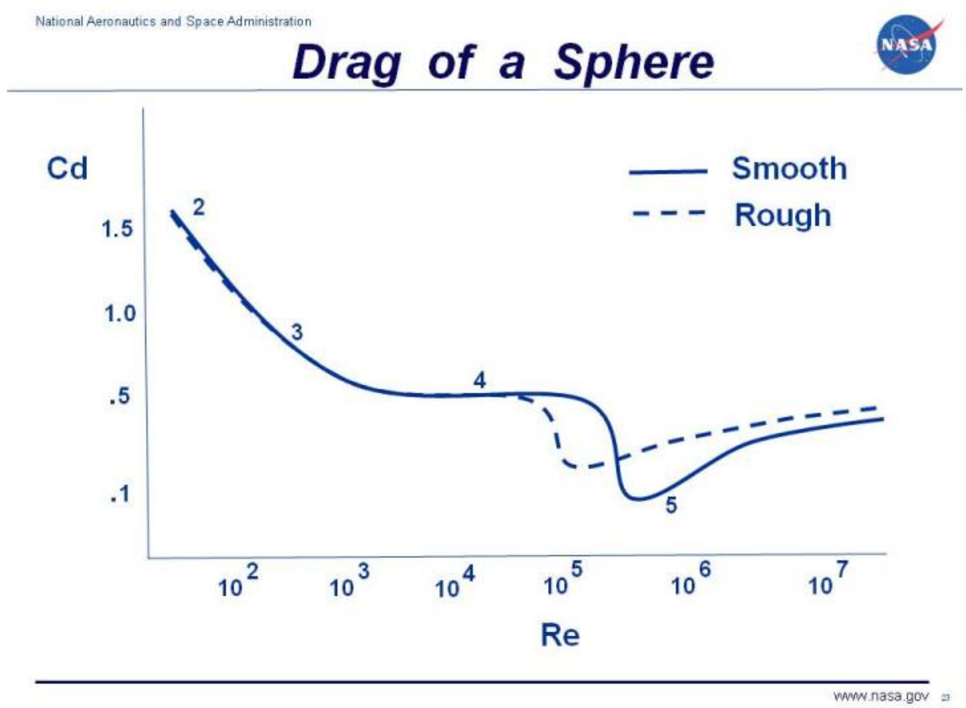

Figure 2. Drag on a Sphere vs. Reynolds Number, with Flow Types Corresponding to Figure 1

Attachment B.[7]

Basic VOF Model Equations

As mentioned in the VOF model description, the former assumes that all immiscible fluid phases present in a control volume share the same velocity, pressure and temperature fields. As a consequence, the same set of basic governing equations describing momentum, mass and energy transport in a single-phase flow (see Modeling Flow Using a Segregated Approach) is solved for an equivalent fluid whose physical properties are calculated as functions of the physical properties of its constituent phases and their volume fractions, e.g.

$$\rho = \sum_i \rho_i \alpha_i \tag{1053}$$

$$\mu = \sum_i \mu_i \alpha_i \tag{1054}$$

$$c_p = \sum_i \frac{(c_p)_i \rho_i}{\rho} \alpha_i \tag{1055}$$

where

$$\alpha_i = \frac{V_i}{V}$$

is the volume fraction and ρ_i, μ_i and $(c_p)_i$ are the density, molecular viscosity and specific heat of the *i* th phase.

The transport of volume fractions α_i is described by the following conservation equation:

$$\frac{d}{dt}\int_V \alpha_i dV + \int_S \alpha_i(\boldsymbol{v} - \boldsymbol{v}_g) \cdot d\boldsymbol{a} = \int_V s_{\alpha_i} dV \tag{1056}$$

where s_{α_i} is the source or sink of the *i* th phase.

In the case of a large time variation of phase volume fractions α_i there is a large time variation of the mixture density ρ which features in the continuity equation, Eqn. (112). Since this unsteady term cannot be linearized in terms of pressure and velocity, it acts as a large source term which can be "unpleasant" for a numerical treatment within a segregated solution algorithm. Because of this, Eqn. (112) is rearranged in the following, non-conservative form:

$$\int_A \mathbf{v} \cdot d\mathbf{a} = \sum_i \int_V \left(s_{\alpha_i} + \frac{\alpha_i}{\rho_i} \frac{D\rho_i}{Dt} \right) dV \tag{1057}$$

where $D\rho_i/Dt$ is the material or Lagrangian derivative of the phase densities ρ_i. One can see that in the case when phases have constant densities and have no sources, the continuity equation reduces to $\nabla \cdot \mathbf{v} = 0$.